SCIENTIFIC REPORTS

OPEN

A new route to enhance the ferromagnetic transition temperature in diluted magnetic semiconductors

Received: 9 May 2017
Accepted: 28 July 2017
Published online: 29 August 2017

Kalpataru Pradhan[1] & Subrat K. Das[2]

We investigate the magnetic and the transport properties of diluted magnetic semiconductors using a spin-fermion Monte-Carlo method on a simple cubic lattice in the intermediate coupling regime. The ferromagnetic transition temperature T_c shows an optimization behavior with respect to the absolute carrier density p_{abs} and the magnetic impurity concentration x as seen in the experiments. Our calculations also show an insulator-metal-insulator transition across the optimum p_{abs} where the T_c is maximum. Remarkably, the optimum p_{abs} values lie in a narrow range around 0.11 (holes/site) for all x values and the ferromagnetic T_c increases with x. We explain our results using the polaron percolation mechanism and outline a new route to enhance the ferromagnetic transition temperature in experiments.

Diluted magnetic semiconductors (DMS) are materials of strong interest due to both, their novel ferromagnetism and potentiality for future spintronics[1–5]. In particular, $Ga_{1-x}Mn_xAs$[6,7,8] with ferromagnetic transition temperature $T_c \simeq 191$ K in films[9] and even more ($\simeq$200 K)[10] in nano wires has led intensive efforts to increase T_c in view of possible technological applications.

It is widely accepted that S = 5/2 Mn^{2+} ion replaces Ga^{3+} ion in $Ga_{1-x}Mn_xAs$ and thereby contributes a hole to the semiconductor valence band, which mediate the magnetic interaction between the localized spins. However, point defects like Mn interstitials (Mn_I) and As antisites[11,12] significantly compensate the free hole density. In addition, Mn_I are highly mobile and preferentially choose the interstitial positions adjacent to Ga substituted Mn ions (Mn_{Ga}), thus forming anti-ferromagnetic $Mn_{Ga} - Mn_I$ pairs[13] and consequently increases the Mn inactive sites. So, overall Mn_I reduces the hole density and the effective Mn concentration (x_{eff}) to Mn_{Ga}-2Mn_I and Mn_{Ga}-Mn_I, respectively, hindering the higher ferromagnetic T_c in (Ga,Mn)As. We define the carrier density $p = p_{abs}/x$, where x is the Mn concentration and p_{abs} is the absolute carrier density. So in this paper p_{abs} denotes *holes per each site*, while p denotes *holes per each impurity site*. The p_{abs} in our language is similar to the hole density (holes per cm^3) generally reported in the experiments.

Most of the experimental studies have been devoted in the search of room-temperature ferromagnetism using different methods. Post-growth annealing is one of the most extensively used technique which enhances the T_c by reducing the Mn_I concentration and in turn increasing the carrier concentration[14]. It is important to note that all Mn_I can not be removed from the sample[15]. Even after the annealing 20% of the Mn impurities remain at the interstitial positions for $x \approx 0.1$, putting a limit to the T_c which either saturates or decreases at larger x[16,17]. Consequently, the system goes from insulating to metallic and then again to insulating phase with x[18].

Another route to enhance the T_c is by co-doping p-type or n-type dopants that can tune the hole density. The enhancement of T_c depends upon x and type of the co-dopant. It is observed that Be (p-type co-dopant) co-doping in $Ga_{1-x}Mn_xAs$ increases both the hole density and the T_c for magnetic impurity concentration $x = 0.03$ [ref. 19]. On the other hand, for $x = 0.05$ the hole density either saturates or decreases due to the increase in Mn_I concentration and as a result T_c decreases[19,20]. In contrast, Si (n-type co-dopant) co-doping decreases the hole density for all values of x [refs 21 and 22]. In this case, for $x \leq 0.08$ T_c decreases as compared to the un-codoped ones, but for higher x (>0.08) Si co-doping increases the T_c. Now, if we focus on the enhancement of T_c and

[1]CMP Division, Saha Institute of Nuclear Physics, HBNI, Kolkata, 700064, India. [2]SKCG Autonomous College, Paralakhemundi, Odisha, 761200, India. Correspondence and requests for materials should be addressed to K.P. (email: kalpataru.pradhan@saha.ac.in)

summarize the experimental results then in the low impurity concentration regime ($x \leq 0.08$) if the hole density increases, with co-doping, the ferromagnetic T_c increases. And, in the higher impurity concentration regime the ferromagnetic T_c increases with decrease in the hole density as compared to the un-codoped samples.

It is believed that it is necessary to increase effective Mn concentration to enhance the T_c[8], but T_c decreases beyond $x_{eff} = 0.07$ [ref. 17]. So it is important to search a route in which both the Mn concentration and the hole density can be altered using growth and post-growth techniques. In this report, we investigate this scenario and outline a procedure to enhance T_c with Mn impurity concentration x. We calculate the ferromagnetic T_c within a diluted Kondo lattice model in the intermediate coupling regime using a Monte-Carlo technique based on travelling cluster approximation[23] on large size systems. The ferromagnetic T_c shows an optimization behavior with x and p_{abs}, and in the process system undergoes an insulator-metal-insulator transition. Our results qualitatively agree with the recent experiments. We find that optimum p_{abs}, where T_c is maximum, lies around 0.11 for a wide range of $x = 0.1$–0.35. And, for a fixed p_{abs} ferromagnetic T_c increases with x, which suggests a new pathway to achieve high temperature DMS.

Model Hamiltonian

We consider a diluted Kondo lattice Hamiltonian[24–26] on a simple cubic lattice:

$$H = -t \sum_{\langle ij \rangle \sigma} (c^{\dagger}_{i\sigma} c_{j\sigma} + h.c.) - \frac{J}{2} \sum_{R} \mathbf{S}_R \cdot \vec{\sigma}_R - \mu \sum_{i} c^{\dagger}_{i\sigma} c_{i\sigma},$$

where $c^{\dagger}_{i\sigma}$ ($c_{i\sigma}$) are the fermion creation (annihilation) operators at site i with spin σ and t is the nearest neighbor ($\langle ij \rangle$) hopping parameter. The second term represents the Hund's coupling J between the localized impurity spin $\mathbf{S}_R$ and the itinerant electrons $\vec{\sigma}_R$ (represented by Pauli spin matrices) at random site R. The itinerant electrons mediates an indirect interaction between the localized spins $\mathbf{S}_R$. As the magnetic moment $S_R = 5/2$, in this paper, we considered the spin $\boldsymbol{S}_R$ to be classical and absorb the magnitude of $\boldsymbol{S}_R$ into J without loss of generality. μ is the chemical potential. Magnetic moment clustering and hence the direct exchange interaction between the localized spins are neglected. In our particle-hole symmetric model the magnetic and transport properties are presented in terms of fixed hole density. In order to get the same hole density throughout the calculations (hole density checked using Fermi-Dirac distribution) we tune the chemical potential μ during the annealing process at each temperature. J is scaled with hopping parameter t. Using a realistic bandwidth $W = 12t = 6$ eV for the host semiconductor GaAs we set $t = 0.5$ eV.

We employ exact diagonalization based Monte-Carlo (ED + MC) approach to anneal the system towards the ground state at fixed density and temperature. In this method the classical spin $\mathbf{S}_R$ is updated at a site and the internal energy is calculated by exact diagonalization of the carriers in the background of the new spin configuration. The proposed update is accepted or rejected by using the classical Monte-Carlo scheme based on Metropolis algorithm. A single system sweep constitutes the above process repeated over each classical spin once. At each temperature one needs at least over 2000 system sweeps to anneal the system sufficiently. But, the exact diagonalization is numerically expensive and grows as $O(N^4)$ per system sweep where N is the number of lattice sites. So, we employ travelling cluster approximation (TCA)[23,27] to handle system size as large as $N = L^3 = 10^3$. In TCA, the Monte-Carlo scheme is implemented by diagonalizing a Hamiltonian reconstructed from a cluster around the to-be-updated site rather than diagonalizing the full lattice. The cost of computation for system sweep reduces to $O(N \times N_c^3)$ for a cluster size N_c. We use a cluster size $N_c = 4^3$ in our calculations. All physical quantities are averaged over ten different randomly localized spin configurations.

Results and Discussion

We start our calculations for different J values with a specific choice of $x = 0.25$ and $p = 0.5$ which is a good starting point for simple cubic lattice. A simple cubic lattice has one atom per unit cell, where as GaAs is face centered cubic with four atoms per unit cell. So, roughly 25% of x in our case corresponds to 6.25% that in real experiments. Magnetic and transport properties in DMS are the consequence of the competition between the carrier mediated ferromagnetic spin-spin interaction and the carrier localization. For $J \sim 0$ there is no carrier mediated spin-spin interaction and as a result there is no ferromagnetism. A minimum value of J is required to generate the ferromagnetic interaction which also depends upon x and p. As J increases from a smaller value ferromagnetic ordering starts to develop. Further, at larger J the carriers get trapped in spin impurity sites and the ferromagnetism is suppressed. So the optimal T_c lies in the intermediate range of J as shown in Fig. 1(a). The carrier localization for higher J is apparently clear from the the developments of an impurity like band in the density of states $N(\omega) = \left\langle \frac{1}{N} \sum_{\alpha} \delta(\omega - \varepsilon_{\alpha}) \right\rangle$ at relatively high temperature $T = 290$ K as shown in Fig. 1(b). The ferromagnetic T_c is estimated from the spin-spin correlation function $S(\mathbf{q}) = \frac{1}{N} \sum_{ij} \mathbf{S_i} \cdot \mathbf{S_j} e^{i\mathbf{q}\cdot(\mathbf{r_i} - \mathbf{r_j})}$, where the ferromagnetic order is indicated by a peak at wave vector $\mathbf{q} = \mathbf{0}$. In Fig. 1(c) we plot the ferromagnetic structure factor $S(\mathbf{0})$ vs temperature for $J/t = 5$, $x = 0.25$, and $p = 0.5$. The inset shows that $S(\mathbf{0})$ for $L = 8$ and $L = 10$ are barely distinguishable at T_c. So we have considered $L = 8$ for rest of our calculations.

We obtain the resistivity for different J values by calculating the *dc* limit of the conductivity determined by the Kubo-Greenwood formula[28,29] as shown in Fig. 1(d). At low temperature the system shows metallic behavior for small and intermediate J values. As J increases ($J/t = 7$) the system remains insulating in the whole temperature range due to carrier localization at impurity sites. For rest of our calculations we use intermediate coupling strength $J/t = 5$ where T_c is found to be maximum and relevant to DMS. Temperature dependence of the ferromagnetic structure factor and the resistivity [see Fig. 1(c)] show one-to-one correspondence between the onset of the ferromagnetism and the metalicity at $T_c \sim 200$ K.

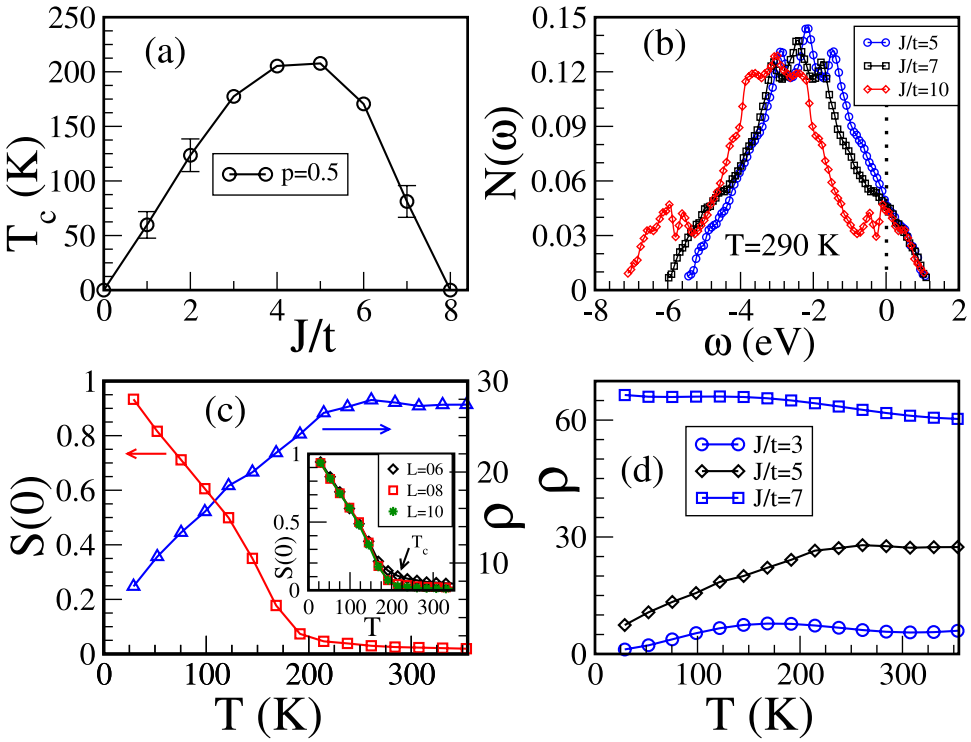

Figure 1. (**a**) Shows optimization behaviour of ferromagnetic T_c with J/t for fixed $p = 0.5$; (**b**) density of states $N(\omega)$ showing the formation of an impurity band for $J/t = 7$ and 10 at $T = 290$ K. Fermi energy is set at zero; (**c**) temperature dependence of the ferromagnetic structure factor $S(\mathbf{0})$ and resistivity in units of $\hbar a/\pi e^2$ (a is lattice constant) for fixed $J/t = 5$ and $p = 0.5$. This shows the onset of ferromagnetism and metalicity at the same temperature. Inset: ferromagnetic structure factor $S(\mathbf{0})$ vs temperature for three different lattice sizes $L = 6$, 8, and 10 where T_c (indicated by arrow) is hardly distinguishable for $L = 8$ and 10; (**d**) temperature dependence of the resistivity (in units of $\hbar a/\pi e^2$) for $J/t = 3$, 5, and 7 showing a metal-insulator transition with increasing J/t.

In carrier-mediated magnetic systems a minimum amount of carrier is essential to initiate the coupling between the magnetic spins, which depends on J/t and x. On the other hand, for higher carrier density the magnetism is suppressed due to decrease in carrier mobility. The overall behavior of T_c with p is shown in Fig. 2(a) for $J = 5$ and $x = 0.25$. The mobility picture is confirmed from the conductivity calculation, where T_c and the conductivity (at the low temperature) are maximized at $p = 0.45$ (see the inset). In order to compare our result with the experiment we plot the data from ref. 17 in Fig. 2(b) such that the impurity concentrations x lie in a narrow range from 0.025–0.035 which we assume to be nearly constant. Now, if we match, the T_c vs p behavior in the experiment is very similar to our results. A metal-insulator transition with p is also observed in the same experiment (not shown here) which we already illustrated the inset of Fig. 2(a).

The carrier mobility and hence the ferromagnetism can be tuned with J, p or x independently. The carrier-spin interaction J is only operative at the impurity sites i.e. for fixed J value the effective coupling strength of the system increases with impurity concentration x. This is similar to the case of increasing J with keeping x fixed. So the variation of T_c with x for fixed p values [Fig. 2(c)] can be understood from the T_c dependence of J/t as in Fig. 1(a). We plot the experimental data from the ref. 17 in Fig. 2(d) such that the carrier densities p lie in a narrow range from 0.86–0.93. We have neglected this small variation of p for qualitative comparison with our calculations and find that the T_c shows an optimization behavior with x, quite similar to our results. It is important to note that if we increase both x and p along the arrow shown in Fig. 2(c) the T_c increases, which mimics the effect of post-growth annealing on T_c. Our calculated T_c values in Fig. 2(a,c) are higher than the experimental T_c values [in Fig. 2(b,d)] due to the higher impurity concentrations used in our calculations.

Figure 3(a) shows the ferromagnetic windows for various values of x in a wide range starting from as small as 10%. We find that the optimal p value where the T_c is maximum decreases with x, which is in contrast to the earlier claim where $p = 0.5$ is suggested to be the optimum value irrespective of impurity concentrations[24]. Further, our results explain the experimental findings where both x and p can be changed simultaneously. In experiments, it is observed if p decreases with co-doping then for high (low) impurity concentration x the ferromagnetic T_c increases (decreases)[21,30]. To compare our results with the experiment we focus around $p = 0.4$, the dotted line in Fig. 3(a). Now, if we decrease p the transition temperature decreases for lower values of x (=0.25 and 0.20) but increases for higher values like $x = 0.30$ and 0.35, which captures the experimental results discussed above. Our calculations clearly demonstrate that T_c can be increased with x provided the p value is tuned properly but not arbitrarily. For $x = 0.1$ and $t = 0.5$ eV the estimated T_c is 120 K, which matches reasonably well with the experiments[18].

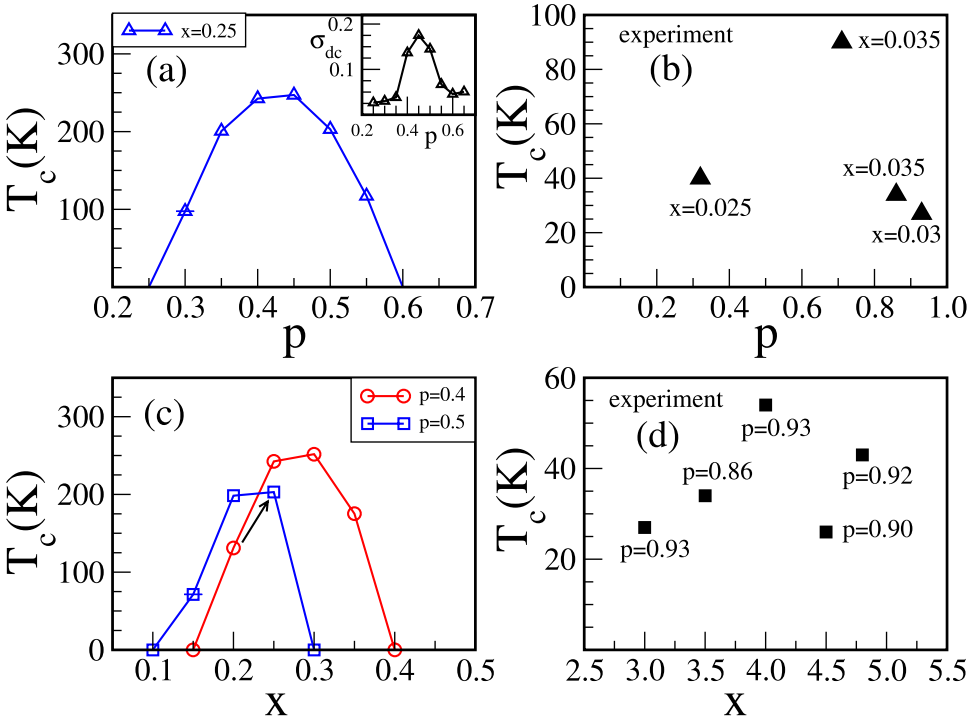

Figure 2. For fixed $J/t = 5$: (**a**) plots p dependence of the ferromagnetic T_c and (inset) the *dc* conductivity in units of $\pi e^2/\hbar a$ calculated at T = 29 K for fixed $x = 0.25$. It shows the correlation between the ferromagnetic T_c and the carrier mobility; (**c**) variation of the ferromagnetic T_c with x for $p = 0.4$ and 0.5. The arrow mimics the effect post-growth annealing on T_c; (**b**,**d**) shows the experimental results (ref. 17) on ferromagnetic T_c vs p and x, respectively.

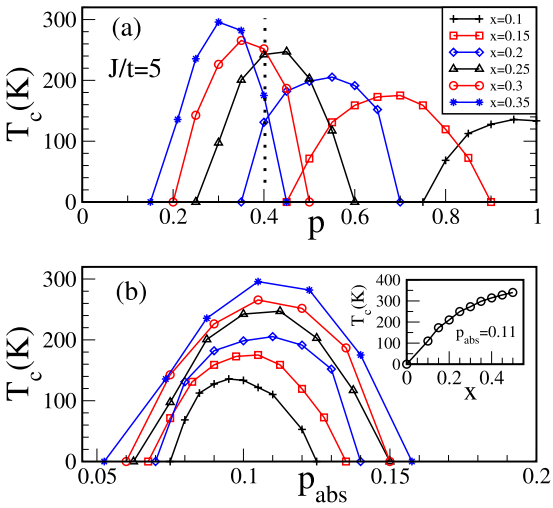

Figure 3. Ferromagnetic windows in terms of the ferromagnetic T_c vs (**a**) the hole density p and (**b**) the absolute hole density p_{abs} for different impurity concentrations x for fixed $J/t = 5$. The symbols for different x values in (**b**) are the same as in (**a**). Inset: x dependence of ferromagnetic T_c for fixed $p_{abs} = 0.11$ showing an increase in T_c with x.

It is generally believed that the p value must be maximized to obtain a higher ferromagnetic T_c in DMS. In Fig. 3(a) our calculations show otherwise, the optimum p value decreases with increasing x. To interpret our finding, in Fig. 3(b), we re-plot the ferromagnetic windows in terms of the absolute carrier density p_{abs} as defined earlier. Interestingly, we find that the ferromagnetic windows lie on top of each other with optimum p_{abs} around 0.11 for $x = 0.35$, which decreases slightly for smaller x values. To understand this we start our discussion from the double exchange (large J) limit where carrier spins are aligned in the direction of the core spin. For $x = 1$ (spins at each site) carriers get delocalized and the electronic kinetic energy is minimized for the ferromagnetic ground

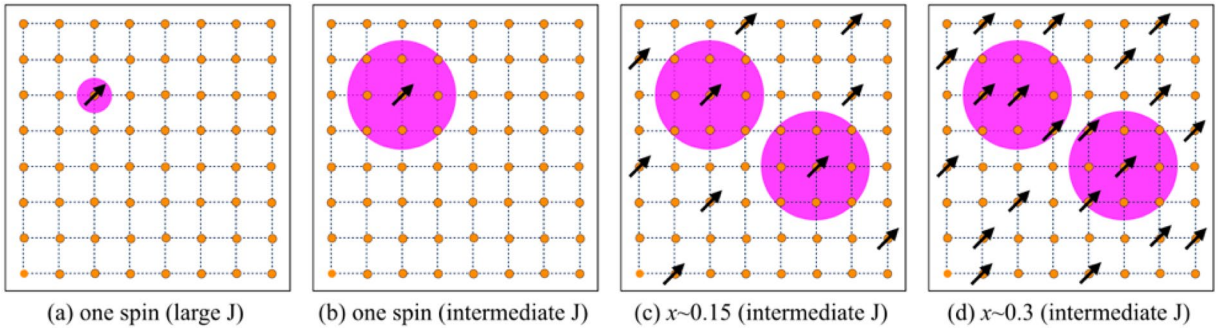

Figure 4. 2D Schematics show the electron delocalization picture by the shaded regions (polarons) for four different cases (arrow indicate the impurity spin); (**a**) localized polaron in the double exchange limit (large J/t) and (**b**) extended polaron in intermediate coupling regime for one spin and one electron case; extended polarons are shown in the intermediate coupling regime for two different diluted limits (**c**) $x = 0.15$ and (**d**) $x = 0.3$.

state in the range $0 < p_{abs} < 1$, where the optimum ferromagnetic T_c is found to be at $p_{abs} = 0.5$ [ref. 31]. This we call the optimum p_{abs}. The range of ferromagnetic ground state is confined to $0 < p_{abs} < 0.3$ in the intermediate coupling regime and the optimum p_{abs} decreases to ~0.15 [ref. 32]. In the diluted limit ($x = 0.1$–0.35) we find [see Fig. 3(b)] that the optimum p_{abs} value is ~0.11 which is in the right ball park as compared to the $x = 1$ limit. This can be understood within a polaron picture discussed below.

In the double exchange limit for one spin and one carrier problem the carrier remains localized to the core spin. A single site localized polaron is shown schematically as the shaded region in Fig. 4(a). In the intermediate coupling regime the carrier delocalization extends over many lattice sites as shown in Fig. 4(b). For a given x a minimum concentration of polarons is required for ferromagnetic percolation. For $x = 0.15$ the ferromagnetic window starts at $p_{abs} \simeq 0.07$ and T_c is maximum for $p_{abs} \simeq 0.10$. When we increase x the optimum p_{abs} does not change in the range $x = 0.1$–0.35, studied in this paper. This indicates that the number of spins in the shaded region increases without affecting the polaron size, schematically shown in Fig. 4(c,d). Now, if we plot T_c vs x for $p_{abs} = 0.11$ then T_c increases with x in the diluted limit and saturates for concentrated x values [see the inset of Fig. 3(b)].

Using the insight obtained from our calculations we suggest a two step procedure to enhance the ferromagnetic T_c in experiments. The first step is to determine the optimum carrier density p_{abs} for a fixed impurity concentration x. So in this step one needs to tune p_{abs} without changing x, which can be achieved by using an external process like hydrogenation[33,34]. After extracting the optimal p_{abs} the second step is to increase only x without altering the optimal p_{abs} value obtained in the first step. With increasing x the p_{abs} would change too, which can be tuned back to its optimal value by co-doping with suitable (n-type or p-type) element. It is important to note that co-doping not only tunes the hole density but also increases the effective x[35,36] and will be helpful to enhance the T_c further. We believe that a systematic combination of experimental processes *e.g.* doping, annealing, hydrogenation, and co-doping can be designed to prepare DMS with higher T_c.

Conclusion

In conclusion, our model calculations provide a new framework to increase the ferromagnetic T_c in diluted magnetic semiconductors. The optimum p_{abs} (absolute carrier density), where T_c is maximum, lies around 0.11 and T_c increases with x for fixed p_{abs} in a broad range of x studied in this letter. To replicate such a scenario in the experiment, p_{abs} has to be determined for small x and then effort should be made to increase x without altering the p_{abs} value. This procedure, viable in experiments, would enhance the ferromagnetic T_c. We hope that our finding will motivate new experiments by combining the growth and the post-growth process outlined here to achieve high T_c DMS for spintronics applications.

References

1. Munekata, H. *et al.* Diluted magnetic III–V semiconductors. *Phys. Rev. Lett.* **63**, 1849 (1989).
2. Ohno, H. Making Nonmagnetic Semiconductors Ferromagnetic. *Science* **281**, 951 (1998).
3. Jungwirth, T., Sinova, J., Masek, J., Kucera, J. & MacDonald, A. H. Theory of ferromagnetic (III, Mn)V semiconductors. *Rev. Mod. Phys.* **78**, 809 (2006).
4. Dietl, T. More than just room temperature. *Nature Mater.* **9**, 965 (2010).
5. Dietl, T. & Ohno, H. Dilute ferromagnetic semiconductors: Physics and spintronic structures. *Rev. Mod. Phys.* **86**, 187 (2014).
6. Ohno, H. *et al.* Ga, Mn)As: A new diluted magnetic semiconductor based on GaAs. *Appl. Phys. Lett.* **69**, 363 (1996).
7. Dietl, T., Ohno, H., Matsukura, F., Cibert, J. & Ferrand, D. Zener Model Description of Ferromagnetism in Zinc-Blende Magnetic Semiconductors. *Science* **287**, 1019 (2000).
8. Jungwirth, T. *et al.* Prospects for high temperature ferromagnetism in (Ga, Mn)As semiconductors. *Phys. Rev. B* **72**, 165204 (2005).
9. Chen, L. *et al.* Low-temperature magnetotransport behaviors of heavily Mn-doped (Ga, Mn)As films with high ferromagnetic transition temperature. *Appl. Phys. Lett.* **95**, 182505 (2009).
10. Chen, L. *et al.* Enhancing the Curie Temperature of Ferromagnetic Semiconductor (Ga, Mn)As to 200 K via Nanostructure Engineering. *Nano Lett.* **11**, 2584 (2011).
11. Yu, K. M. *et al.* Curie temperature limit in ferromagnetic $Ga_{1-x}Mn_xAs$. *Phys. Rev. B* **65**, 201303(R) (2002).
12. Myers, R. C. *et al.* Antisite effect on hole-mediated ferromagnetism in (Ga, Mn)As. *Phys. Rev. B* **74**, 155203 (2006).

13. Blinowski, J. & Kacman, P. Spin interactions of interstitial Mn ions in ferromagnetic GaMnAs. *Phys. Rev. B* **67**, 121204(R) (2003).
14. Potashnik, S. *et al*. Effects of annealing time on defect-controlled ferromagnetism in $Ga_{1-x}Mn_xAs$. *Appl. Phys. Lett.* **79**, 1495 (2001).
15. Edmonds, K. W. *et al*. Mn Interstitial Diffusion in (Ga, Mn)As. *Phys. Rev. Lett.* **92**, 037201 (2004).
16. Potashnik, S. J. *et al*. Saturated ferromagnetism and magnetization deficit in optimally annealed $Ga_{1-x}Mn_xAs$ epilayers. *Phys. Rev. B* **66**, 012408 (2002).
17. Dobrowolska, M. *et al*. Controlling the Curie temperature in (Ga, Mn)As through location of the Fermi level within the impurity band. *Nature Mater.* **11**, 444 (2012).
18. Matsukura, F., Ohno, H., Shen, A. & Sugawara, Y. Transport properties and origin of ferromagnetism in (Ga, Mn)As. *Phys. Rev. B* **57**, R2037(R) (1998).
19. Lee, S., Chung, S. J. & Choi, I. S. Effect of Be doping on the properties of GaMnAs ferromagnetic semiconductors. *J. Appl. Phys.* **93**, 8307 (2003).
20. Yu, K. M. *et al*. Curie temperature limit in ferromagnetic $Ga_{1-x}Mn_xAs$. *Phys. Rev. B* **68**, 041308(R) (2003).
21. Cho, Y. J., Yu, K. M., Liu, X., Walukiewicz, W. & Furdyna, J. K. Effects of donor doping on $Ga_{1-x}Mn_xAs$. *Appl. Phys. Lett.* **93**, 262505 (2008).
22. Kim, H. C., Khym, S., Lee, S., Liu, X. & Furdyna, J. K. Magnetic anisotropy of $Ga_{1-x}Mn_xAs$ films with additional nonmagnetic donor doping. *J. Appl. Phys.* **107**, 09C303 (2010).
23. Kumar, S. & Majumdar, P. A travelling cluster approximation for lattice fermions strongly coupled to classical degrees of freedom. *Eur. Phys. J. B* **50**, 571 (2006).
24. Alvarez, G., Mayr, M. & Dagotto, E. Phase Diagram of a Model for Diluted Magnetic Semiconductors Beyond Mean-Field Approximations. *Phys. Rev. Lett.* **89**, 277202 (2002).
25. Chattopadhyay, A., Das Sarma, S. & Millis, A. J. Transition Temperature of Ferromagnetic Semiconductors: A Dynamical Mean Field Study. *Phys. Rev. Lett.* **87**, 227202 (2001).
26. Berciu, M. & Bhatt, R. N. Effects of Disorder on Ferromagnetism in Diluted Magnetic Semiconductors. *Phys. Rev. Lett.* **87**, 107203 (2001).
27. Pradhan, K., Mukherjee, A. & Majumdar, P. Distinct Effects of Homogeneous Weak Disorder and Dilute Strong Scatterers on Phase Competition in Manganites. *Phys. Rev. Lett.* **99**, 147206 (2007).
28. Mahan, G. D. *Quantum Many Particle Physics* (Plenum Press, New York, 1990).
29. Kumar, S. & Majumdar, P. Transport and localisation in the presence of strong structural and spin disorder. *Eur. Phys. J. B* **46**, 237 (2005).
30. Wang, W. Z. *et al*. Influence of Si doping on magnetic properties of (Ga, Mn)As. *Physica E* **41**, 84 (2008).
31. Yunoki, S. *et al*. Phase Separation in Electronic Models for Manganites. *Phys. Rev. Lett.* **80**, 845 (1998).
32. Pradhan, K. & Majumdar, P. Magnetic order beyond RKKY in the classical Kondo lattice. *Euro. Phys. Lett.* **85**, 37007 (2009).
33. Thevenard, L., Largeau, L., Mauguin, O. & Lemaitre, A. Tuning the ferromagnetic properties of hydrogenated GaMnAs. *Appl. Phy. Lett.* **87**, 182506 (2005).
34. Goennenwein, S. T. B. *et al*. Hydrogen Control of Ferromagnetism in a Dilute Magnetic Semiconductor. *Phys. Rev. Lett.* **92**, 227202 (2004).
35. Fujii, H., Sato, K., Bergqvist, L., Dederichs, P. H. & Katayama-Yoshida, H. Interstitial Donor Codoping Method in (Ga, Mn)As to Increase Solubility of Mn and Curie Temperature. *Appl. Phys. Express* **4**, 043003 (2011).
36. Bergqvist, L., Sato, K., Katayama-Yoshida, H. & Dederichs, P. H. Computational materials design for high-Tc (Ga, Mn)As with Li codoping. *Phys. Rev. B* **83**, 165201 (2011).

Acknowledgements

We acknowledge use of TCMP computer cluster at SINP and our discussion with Pinaki Majumdar.

Author Contributions

Numerical Calculations: K.P.; interpretation and manuscript writing: K.P. and S.K.D.

Additional Information

Competing Interests: The authors declare that they have no competing interests.

Publisher's note: Springer Nature remains neutral with regard to jurisdictional claims in published maps and institutional affiliations.